Electronic Supplementary Information

Realization of Dehydrogenation Pathway of Formic Acid Oxidation by Ultra-Small Core-Shell Au-Pt Nanoparticles with Discrete Pt Shells

Yi Cao,[a,§] Xiang Zhang,[a,§] Xinru Yue,[a] Mengmeng Zhang,[a] Wei Du,[b] Haibing Xia[a,*]

[a] State Key Laboratory of Crystal Materials, Shandong University, Jinan, 250100, P. R. China.

[b] School of Environment and Material Engineering, Yantai University, Yantai 264005, P. R. China.

§ These authors contributed equally.

E-mail: hbxia@sdu.edu.cn

Experimental section

1. Materials.

Hydrogen tetrachloroaurate(III) tetrahydrate ($HAuCl_4 \cdot 4H_2O$), trisodium citrate dihydrate ($Na_3C_6H_5O_7 \cdot 2H_2O$, 99%), iron(II) sulfate heptahydrate ($FeSO_4 \cdot 7H_2O$, 99%+), concentrated sulfuric acid (H_2SO_4, 95%), and formic acid (HCOOH, 88%) were purchased from Sinopharm Chemical Reagent Co. Ltd. Potassium tetrachloroplatinate(II) (K_2PtCl_4, 99%) was purchased from Alfa Aesar (Shanghai, China). Commercial Pt/C catalysts (20 wt%) was obtained from Johnson Matthey in England. 5 wt % Nafion solution was purchased from Sigma-Aldrich. All chemicals were used as received. All glassware and stirring bars were cleaned with aqua regia (3 : 1 v/v HCl (37%) : HNO_3 (65%) solutions) and then rinsed thoroughly with H_2O before use. (Caution: aqua regia solutions are dangerous and should be used with extreme care; never store these solutions in closed containers.) The water used in all experiments was Milli-Q water (18 MΩ cm, Millipore). The aqueous solution of $HAuCl_4$ (1wt%) and K_2PtCl_4 (1wt%) were prepared and stored at ca. 4 °C before use.

2. Characterization.

Low-resolution transmission electron microscopy (TEM) and high-resolution transmission electron microscopy (HRTEM) images were obtained on a transmission electron microscope operating at an acceleration voltage of 200 kV (JEOL JEM 2100F). Elemental mapping images were acquired by energy dispersive X-ray spectroscopy (EDS) using a JEOL JEM 2100F electron microscope equipped with a STEM unit. X-ray photoelectron spectroscopy (XPS) measurements were carried out on a Thermo Fisher Scientific Escalab 250 XPS spectrometer, using Al Kα X-ray radiation for excitation.

3. Electrochemical Measurements.

Electrochemical measurements for FAOR were conducted on a CHI 660D electrochemical workstation with a standard three-electrode system in 0.25 M H_2SO_4 aqueous solution. Glassy carbon electrode (GCE) with 3 mm diameter was used as the working electrode. A platinum wire was used as the counter electrode, and Ag/AgCl (saturated KCl) was used as the reference electrode. The bare GCE was cautiously polished with 0.3 and 0.05 mm alumina powder, followed by washing scrupulously with Milli-Q water and ethanol under ultrasonication and drying at room temperature.

The preparation of the GCE modified by the $USCS_D$ $Au_{61.2}@Au_{27.3}Pt_{11.5}$-NP/C catalysts is as follows. The $USCS_D$ $Au_{61.2}@Au_{27.3}Pt_{11.5}$-NP/C powder was redispersed in 300 μL of Milli-Q water. After sonication of 30 min, 8 μL of the obtained catalyst ink was carefully drop-coated onto the freshly polished bare GCE (0.07 cm^2 in surface area), followed by drying in air. 4 μL of the ethanol solution of Nafion (0.2 wt%) was coated on the surface of the GCE covered with $USCS_D$ $Au_{61.2}@Au_{27.3}Pt_{11.5}$-NP/C catalysts, followed by drying in air. The Pt loading was 4.93 μg_{Pt} cm^{-2}.

For better comparison, the uniform ink of commercial Pt/C catalysts was also prepared by mixing the commercial Pt/C powder with Nafion solution (5 wt%) and Milli-Q water under sonication for 30 min. And the GCE modified by commercial Pt/C catalysts was prepared by the same procedure as above.

Fig. S1 CV curves of commercial Pt/C catalysts (red curve) and USCS $Au_{38.4}@Au_{9.3}Pt_{52.3}$ NP/C catalysts (blue curve) in the presence of N_2-saturated 0.25 M H_2SO_4 containing 1.0 M HCOOH. The current densities are normalized by Pt mass.

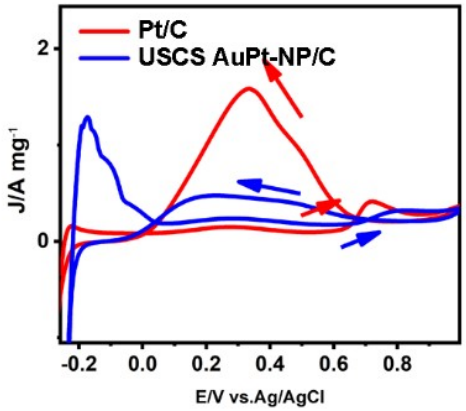

It is known that the oxidation peaks in the potential range of 0.65 to 0.85 V (vs. Ag/AgCl) and 0.05 to 0.65 V indicate the occurrence of FAOR in the direct pathway (dehydrogenation of formic acid) and the indirect pathway (dehydration of formic acid), respectively.[1-3] One can see that during the forward scan, a weak oxidation peak in the potential range of 0.7 to 0.8 V (vs. Ag/AgCl) is observed in the CV curves of commercial Pt/C catalysts (red curve) and USCS AuPt-NP/C catalysts (blue curve). These results indicate that FAOR catalysed by both commercial Pt/C catalysts (red curve) and USCS $Au_{38.4}@Au_{9.3}Pt_{52.3}$ NP/C catalysts in the indirect pathway (the dehydration of formic acid). In addition, the mass-normalized current density of commercial Pt/C catalysts is low, which is a little higher than that of USCS AuPt-NP/C catalysts. These results indicate that their performance towards FAOR are unsatisfactory.

Fig. S2 CV curves of the as-prepared USCS AuPt-NP/C catalysts obtained under different concentrations of Pt(II) ions: 2.43 μM (a),1.95 μM (b),1.70 μM (c) and 1.46 μM (d), which were measured in N_2-satureated 0.25 M H_2SO_4 solution.

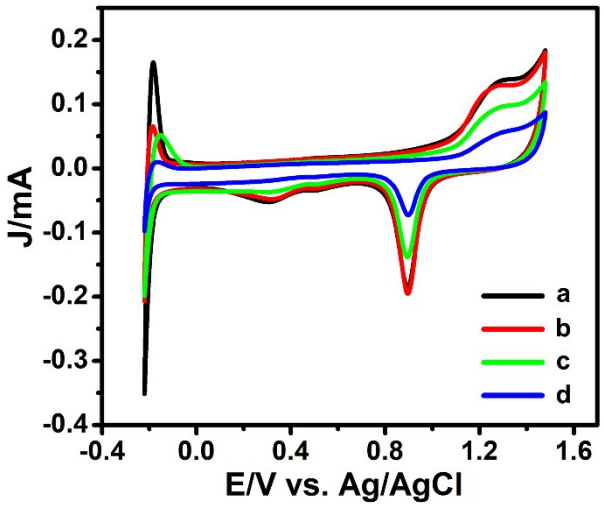

Cyclic voltammetry (CV) curves of $USCS_D$ Au-Pt-NP/C catalysts prepared at different concentrations of Pt(II) (Fig. S2) were measured in N_2-saturated 0.25 M H_2SO_4 solution in the potential range from -0.22 to 1.48 V (vs. Ag/AgCl). On the basis of their CVs, the hydrogen adsorption/desorption region becomes bigger with the increasing concentration of Pt(II) ions from 1.46 to 1.70, 1.95 and 2.43 μM. The results indicate the content of active sites on their surfaces gradually increase. The ECSA values are calculated by measuring the charge collected in the hydrogen adsorption/desorption region after double layer correction and assuming a value of 210 μC cm^{-2} for the adsorption of a hydrogen monolayer. Their ECSA values were calculated accordingly (Table S1).

Fig. S3 CV curve of $USCS_D$ $Au_{61.2}@Au_{27.3}Pt_{11.5}$ NPs measured in the presence of N_2-saturated 0.3 M KOH solution. The area covered by the horizontal line is used to calculate the relative content of Pt and Au on their surface by using the surface charge related to the reduction of oxide species.

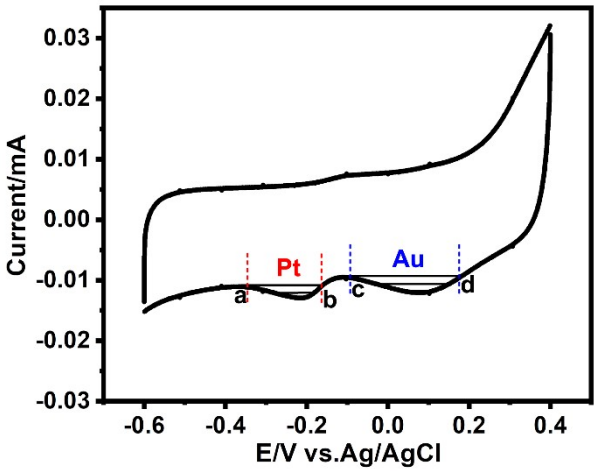

The surface compositions of the as-prepared $USCS_D$ Au-Pt NPs can be calculated on the basis of the surface areas of Au and Pt obtained, which can be deduced as follows:

$$m = \frac{S_{Pt}}{S_{Pt} + S_{Au}} \times 100 \quad (1)$$

$$S_{Pt} = \frac{Q_{Pt}(C)}{543(\mu C cm^{-2})} \quad (2)$$

$$S_{Au} = \frac{Q_{Au}(C)}{493(\mu C cm^{-2})} \quad (3)$$

$$Q_{Pt} = \frac{\int_a^b idE(mAV)}{v(mV/s)} \quad (4)$$

$$Q_{Au} = \frac{\int_c^d idE(mAV)}{v(mV/s)} \quad (5)$$

where *m* represents the ratio of Pt content, and S_{Pt} and S_{Au} are the surface areas covered by Pt and Au oxides, respectively. Moreover, the charge associated to the reduction of oxide species of Pt and Au are 543 μC cm^{-2} and 493 μC cm^{-2} respectively. Furthermore, Q_{Pt} and Q_{Au} are the calculated charge of the surface areas covered by Pt and Au oxides, respectively.

Fig. S4 High-resolution XPS spectra of the Pt 4f signals (a) in USCS $Au_{38.4}@Au_{9.3}Pt_{52.3}$ NPs catalysts and pure Pt NPs catalysts, and the Au 4f signals (b) in USCS $Au_{38.4}@Au_{9.3}Pt_{52.3}$ NPs catalysts and pure Au NPs catalysts.

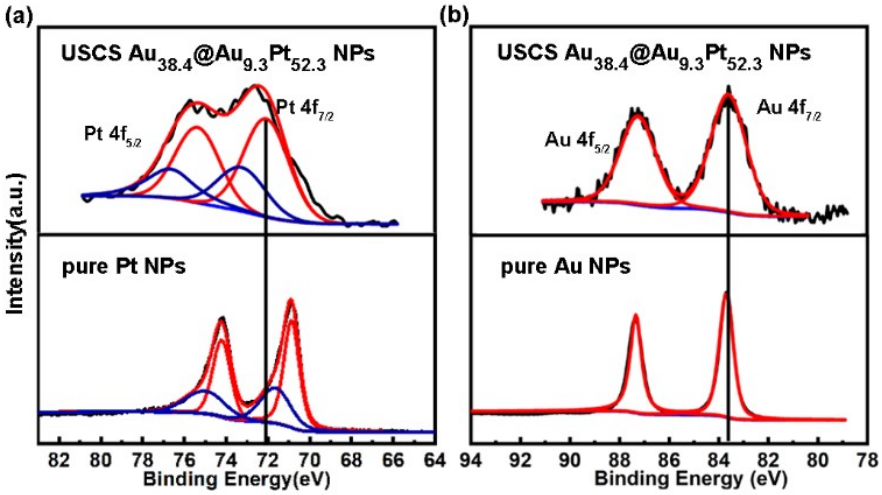

The binding energies (BEs) of Pt $4f_{7/2}$ and Pt $4f_{5/2}$ of USCS $Au_{38.4}@Au_{9.3}Pt_{52.3}$ NPs are 72.1 and 75.4 eV, respectively, which show a positive shift of about 1.2 eV, in comparison with those (70.9 and 74.2 eV) of pure Pt NPs (Fig. S2a). Moreover, BEs of the Au $4f_{7/2}$ and Au $4f_{5/2}$ of USCS $Au_{38.4}@Au_{9.3}Pt_{52.3}$ NPs are 83.6 and 87.2 eV, respectively, which show a slight negative shift of 0.1 eV, compared to those (83.7 and 87.3 eV) of pure Au NPs (Fig. S2b).

Table S1 Summarized data of electrocatalytic performance of a series of $USCS_D$ Au-Pt-NP/C catalysts on FAOR in acidic media. They were prepared the same reaction conditions except the concentration of Pt(II) ions: 2.43 μM (a), 1.95 μM (b), 1.70 μM (c), 1.46 μM (d).

Samples	Pt(II) concentration [μM]	ECSA [m^{-2} g^{-1}]	Mass activity [A mg_{Pt}^{-1}]	Mass activity [A mg_{metal}^{-1}]	Specific activity [mA cm^{-2}]	Peak position [V vs. Ag/AgCl]
a	2.43	184.94	5.12	0.71	2.74	0.32
b	1.95	140.79	6.91	0.79	4.88	0.28
c	1.70	107.87	4.24	0.43	3.92	0.31
d	1.46	68.20	0.98	0.09	1.41	0.26

Table S2 The total composition and surface composition of $USCS_D$ $Au_{61.2}@Au_{27.3}Pt_{11.5}$ NPs by combined analysis of results of EDS and CV curves.

Sample	Total composition		Surface composition		m(Au%)	1-m(Pt%)
	Au(at.%)	Pt(at.%)	Au(at.%)	Pt(at.%)		
$USCS_D$ $Au_{61.2}@Au_{27.3}Pt_{11.5}$ NPs	88.5	11.5	27.3	11.5	70.3	29.7

Table S3 Summarized data of binding energies of Pt 4f signals of $USCS_D$ $Au_{61.2}@Au_{27.3}Pt_{11.5}$-NP/C and commercial Pt/C catalysts.

Sample	Pt(0) $4f_{7/2}$ peak [eV]	Pt(0) $4f_{5/2}$ peak [eV]	ΔPt $4f_{7/2}$ peak [eV]
$USCS_D$ $Au_{61.2}@Au_{27.3}Pt_{11.5}$-NP/C catalysts	71.4	74.5	-0.7
Commercial Pt/C catalysts	72.1	75.2	-

Table S4 Summarized data of binding energies of Au 4f signals of $USCS_D$ $Au_{61.2}@Au_{27.3}Pt_{11.5}$-NP/C catalysts and Au-NP/C catalysts.

Sample	Au(0) $4f_{7/2}$ peak [eV]	Au (0) $4f_{5/2}$ peak [eV]	ΔAu $4f_{7/2}$ peak [eV]
$USCS_D$ $Au_{61.2}@Au_{27.3}Pt_{11.5}$-NP/C catalysts	84.3	88.0	-0.1
Commercial Pt/C catalysts	84.4	88.1	-

Table S5 Comparison in electrocatalytic performance of different Pt-based materials on FAOR reported in literature.

Sample	Mass activity [A mg_{metal}^{-1}]	Specific activity [mA cm^{-2}]	References
$USCS_D$ $Au_{61.2}@Au_{27.3}Pt_{11.5}$-NP/C	6.91	4.88	This work
0.5%Sn/Pt_3Mn	0.13	1.58	J. Catal. 2021, 395, 282–292.[4]
$PtCu_3$ concave nanocubes	0.45	1.57	ACS Appl. Energy Mater. 2020, 3, 1010–1016.[5]
$Pt_{0.05}Au$/C	4.99	-	Int. J. Hydrog. Energy 2020, 45, 16071–16079.[6]
$Pd_{19}Pt_1$ nanosheets	1.8	-	J. Mater. Chem. A 2019, 7, 18846–18851.[7]
Hollow Pt–Ni–Co NDs	~2.2	-	ACS Appl. Energy Mater. 2019, 2, 961–965.[8]
Pt_1Au_1/NG	1.847	-	Chem. Eng. J. 2018, 334, 2638–2646.[9]

References

1 C. Li, Y. Xu, H. Yu, K. Deng, S. Liu, Z. Wang, X. Li, L. Wang and H. Wang, *Nanotechnology*, 2020, **31**, 045401.

2 X. Jiang, X. Yan, W. Ren, Y. Jia, J. Chen, D. Sun, L. Xu and Y. Tang, *ACS Appl. Mater. Interfaces*, 2016, **8**, 31076-31082.

3 X. Hu, J. Zou, H. Gao and X. Kang, *J. Colloid Interface Sci.*, 2020, **570**, 72-79.

4 Y. Li, Y. Wang, S. Li, M. Li, Y. Liu, X. Fang, X. Dai and X. Zhang, *J. Catal.*, 2021, **395**, 282-292.

5 J. Geng, Z. Zhu, X. Bai, F. Li and J. Chen, *ACS Appl. Energy Mater.*, 2020, **3**, 1010-1016.

6 H. Shi, F. Liao, W. Zhu, C. Shao and M. Shao, *Int. J. Hydrogen Energy*, 2020, **45**, 16071-16079.

7 Q. Yang, L. Shi, B. Yu, J. Xu, C. Wei, Y. Wang and H. Chen, *J. Mater. Chem. A*, 2019, **7**, 18846-18851.

8 R. Sriphathoorat, K. Wang and P. K. Shen, *ACS Appl. Energy Mater.*, 2019, **2**, 961-965.

9 H. Xu, B. Yan, S. Li, J. Wang, C. Wang, J. Guo and Y. Du, *Chem. Eng. J.*, 2018, **334**, 2638-2646.